Complex Surface Acoustic Wave Fields used for Microfluidic Applications

Robert Weser[1], Alexandre N. Darinskii[2], Manfred Weihnacht[3], Andreas Winkler[1], and Hagen Schmidt[1]

[1] *Leibniz Institute for Solid State and Materials Research Dresden (IFW Dresden), SAWLab Saxony, 01069 Dresden, Germany, r.weser@ifw-dresden.de*

[2] *Institute of Crystallography FSRC "Crystallography and Photonics," Russian Academy of Sciences, Moscow 119333, Russia*

[3] *InnoXacs – Innovations in Crystal Acoustics, 01744 Dippoldiswalde, Germany*

Introduction

Surface acoustic waves (SAW) are predestined for the active manipulation of fluids as well as of immersed particles or cells in microfluidic lab-on-a-chip systems. The generation of driving forces in the fluid originally rests upon the lateral distribution of the displacement amplitude normal to the substrate surface, i.e. the surface acoustic wave field. Here, we present numerical and experimental results of complex wave field analysis and discuss underlying effects of SAW excitation and propagation on anisotropic, piezoelectric substrates. Furthermore, a novel mechanism for the active manipulation of the polarization of surface acoustic waves is demonstrated that is of particular interest for SAW-driven microfluidics because it enables a more precise control of fluid actuation, and also shows the potential to efficiently reduce losses due to undesirable dissipation of acoustic energy. In general, the combination of theoretical and experimental investigations provides a deeper insight into fundamental effects of acoustofluidic coupling and allows for the realization of tailored SAW-based microfluidic actuators.

SAW-based Microfluidics

The most common way to excite a surface acoustic wave is to utilize an interdigital transducer (IDT) arranged on a piezoelectric substrate. The SAW is excited by applying an alternating electrical voltage to the pair of comb-shaped IDT electrodes giving rise to local vibrations that superimpose to a surface acoustic wave propagating along the substrate surface [1,2]. For microfluidic actuation purposes, the fluid is directly attached to the substrate surface. Hence, a bulk acoustic wave (BAW) is radiated into the fluid which comes along with a transfer of momentum (Fig. 1) that furthermore is used to manipulate immersed objects or even the fluid itself. Note that the transfer of momentum is caused almost exclusively by the surface normal component of SAW displacement amplitude.

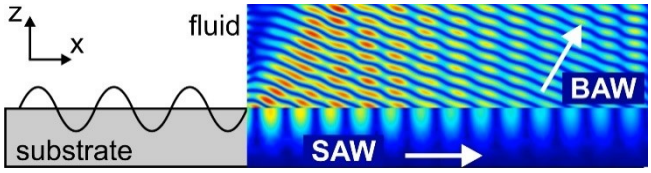

Figure 1: A bulk acoustic wave (BAW) is radiated if the surface acoustic wave (SAW) encounters a fluid region. A transfer of momentum to the fluid takes place, furthermore used to manipulate immersed objects or even the fluid itself.

SAW Propagation on Anisotropic Materials

Fundamentals

Most often, single crystalline piezoelectric, i.e. anisotropic materials are used as substrate. Hence, crystal cut orientation as well as SAW propagation direction with regard to crystal axes are closely related to important parameters of wave excitation and propagation [1]. The phase velocity and polarization of the SAW as well as the coupling coefficient and the power flow angle are of particular interest. Almost all SAW-driven microfluidic devices are fabricated using 128° rotated Y-cut of lithium niobate single crystal with propagation direction along the X-axis (128°YX $LiNbO_3$) due to strong piezoelectric coupling as well as to a dominating normal, i.e. out of plane, component of surface displacement amplitude. Fig. 2 depicts relevant SAW properties of 128°Y $LiNbO_3$ as function of the propagation angle θ, where $\theta = 0$ is equal to SAW propagation parallel to the crystal's X-axis.

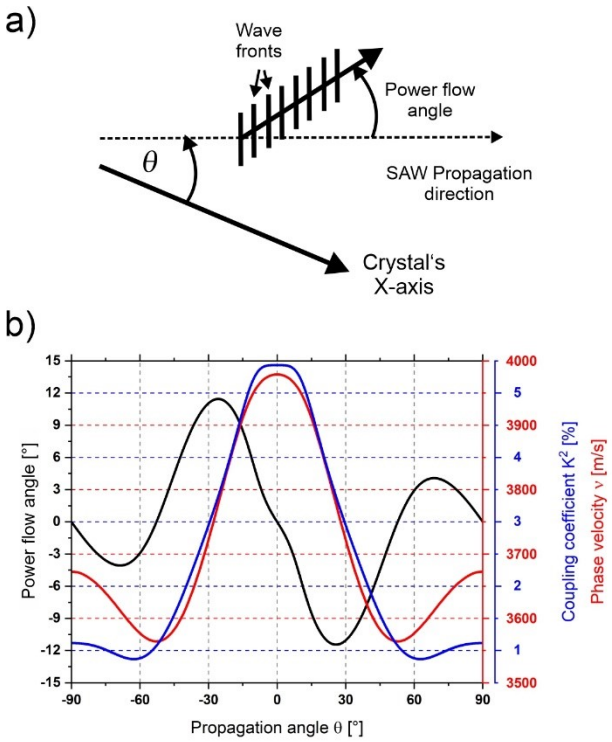

Figure 2: Angular SAW dispersion on 128°Y $LiNbO_3$ (propagation angle with respect to crystal's X-axis): a) description of SAW propagation direction by means of propagation angle $\boldsymbol{\theta}$, b) power flow angle, coupling coefficient, and phase velocity as function of $\boldsymbol{\theta}$.

Investigation of SAW fields

Investigations on SAW excitation were carried out for conventional λ/4 (solid) finger IDTs arranged on 128°Y $LiNbO_3$. The period λ of the IDTs used for microfluidic applications typically is in the range 10 µm to 400 µm, which corresponds to frequencies between 400 MHz and 10 MHz. A single, travelling SAW (tSAW) is excited by one IDT. More complex SAW fields can be achieved by superposition of multiple tSAW, e.g. the formation of standing SAW fields in one or more directions. In this case, several IDTs are arranged at the substrate surface involving significant influence of anisotropy due to their different orientations with respect to the crystal axes.

Considering a SAW propagating along the substrate surface defined by lateral coordinates x and y and surface normal coordinate z, the time-dependent surface displacement $\boldsymbol{u} = (u_x, u_y, u_z)$ at position $(x, y, z = 0)$ is specified by local harmonic oscillations and can be described by linear superposition [1]:

$$\boldsymbol{u}(x,y,t) = \sum_i \boldsymbol{u_i}(x,y,t) = \sum_i \hat{\boldsymbol{u}}_i(x,y) \cdot \cos[\omega_i t + \boldsymbol{\varphi_i}(x,y)] \quad \text{[m]} \qquad (1)$$

where $\hat{\boldsymbol{u}}_i$ denotes the magnitude, $\boldsymbol{\varphi_i}$ a constant phase, and $\omega_i = 2\pi f_i$ the angular frequency of the i^{th} wave contributing to the overall SAW field. Nonlinear effects, arising from e.g. higher order piezoelectric coupling effects or very large amplitudes, are assumed to be neglectable.

Experimental methods

Characterization of the electrical behavior is carried out via electrical *S*-parameter measurements with a vector network analyzer (VNA, Agilent E5071C) yielding frequency dependent, complex electrical admittance/impedance characteristics of IDTs. The lateral distribution of surface normal displacement in terms of amplitude $\widehat{u_z}(x,y)$ and phase $\varphi_z(x,y)$ is measured with a scanning laser Doppler vibrometer (LDV, Polytec UHF 120) [1-3].

Simulation using numerical methods

The aim of simulations is to determine the SAW field on the free surface of the substrate next to the IDT. For a given IDT-substrate combination and a time-harmonic voltage applied to the IDT, the acoustoelectric field is computed using the finite element method (FEM). For this purpose, the stationary equations of piezoacoustics in the substrate material as well as the equations of elastodynamics in the IDT electrodes are solved. Finally, the z-component of mechanical displacement $u_z(x,y)$ on the substrate surface as function of the lateral coordinates x and y is found (see [2] for details of the computational model and its implementation).

Excitation and Propagation of single SAW

Fig. 3 depicts the wave field of a tSAW in front of a single IDT. In case of $\theta = 0$ an almost ideal symmetry with respect to the beam axis ($y = 0$), i.e. perpendicular to the propagation direction, can be observed (Fig. 3a).

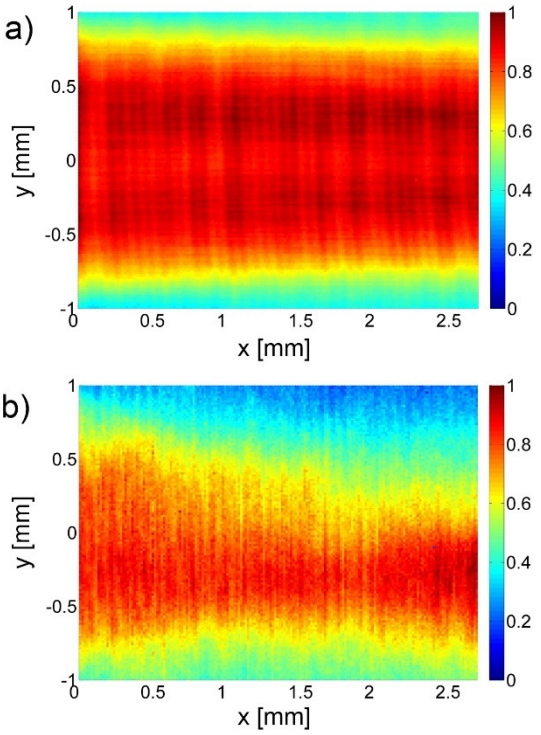

Figure 3: SAW fields in front of single IDT (period λ=150 µm) oriented at different angles $\boldsymbol{\theta}$ w.r.t. to the X-direction. IDT is located at $\boldsymbol{x < 0}$, i.e. SAW propagation direction is from left to right. Magnitude $\widehat{\boldsymbol{u_z}}(\boldsymbol{x},\boldsymbol{y})$ of SAW (scaled to maximum value) measured with LDV for: a) $\boldsymbol{\theta = 0}$ at frequency f=25.74 MHz, b) $\boldsymbol{\theta = 45°}$ at f=23.69 MHz.

No beam steering occurs because the power flow is parallel to the SAW propagation direction. For $\theta = 45°$ no symmetry is observed due to relevant beam steering (Fig. 3b). A negative power flow angle can be observed since the rotation angle of IDT is positive (cf. Fig. 2b). Moreover, maximum displacement amplitude, as given in Fig. 3, appears at different frequencies due to the different SAW phase velocities for both propagation directions at constant IDT period (cf. Fig. 2b). However, the beam profiles indicate a slight focusing effect, i.e. the width of the SAW beam profile decreases with increasing distance from the IDT ($x > 0$), in both cases. This fundamental phenomenon is caused by diffraction effects due to the limited aperture of IDTs.

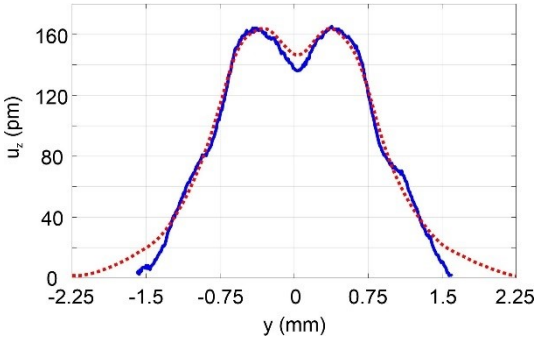

Figure 4: Comparison of measured (LDV measurement, blue) and simulated (FEM-based computation, red) SAW

beam profiles $\boldsymbol{u_z(y)}$ at a distance $\boldsymbol{x = 1.5}$ mm to the IDT (period λ=150 µm, $\boldsymbol{\theta = 0}$, f=25.75 MHz). Equivalent voltage was applied to the IDT during simulation and experiment.

Fig. 4 shows measured and simulated SAW beam profile for the tSAW field from Fig. 3a. Reasonable agreement is observed for both the magnitude and the shape of the profile. Slight discrepancies between theoretically and experimentally determined profiles appear for $|y| > 1.5$ mm that arises from relevant influence of diffraction inside the IDT.

Superposition of multiple SAWs

More complex SAW fields can be realized by superposition of several single SAWs. As an example, Fig. 5 depicts the superposition of four tSAWs that are excited by two orthogonally arranged couples of opposing IDTs. Hence, two counter-propagating tSAWs form a standing SAW in one direction (1DsSAW) and the superposition of both 1DsSAWs finally yields a standing SAW in two directions (2DsSAW). The 2DsSAW field shows a regular pattern, i.e. the amplitude maxima are well-defined and almost uniformly distributed over the entire surface area (Fig. 5a). Moreover, the phase distribution (Fig. 5b) depicts almost pure standing wave behavior indicated by abrupt changes of local phase. Such complex SAW fields are typically used for acoustic tweezer setups, because particles or cells can be trapped at the nodal points of the acoustic field.

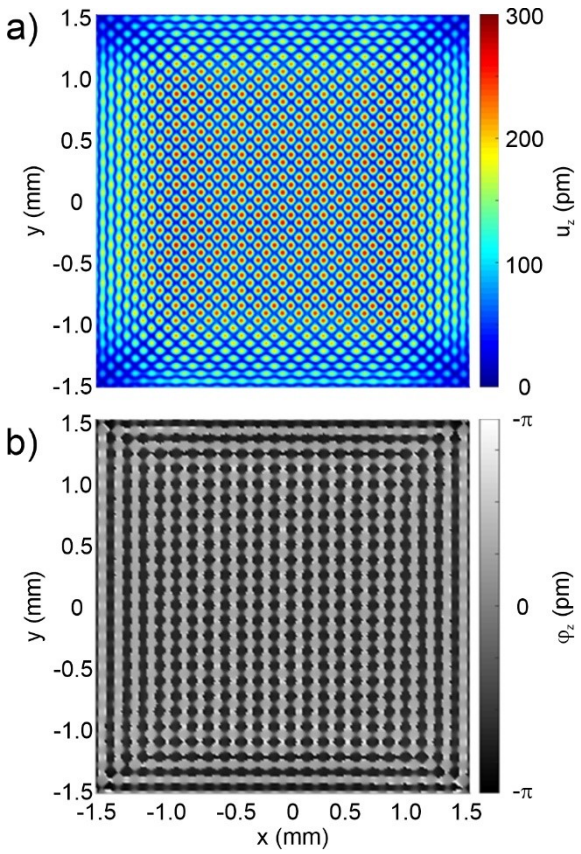

Figure 5: SAW field induced by superposition of four tSAW propagating toward the center ($\boldsymbol{x = y = 0}$). IDTs are located at the edges ($|\boldsymbol{x}| = |\boldsymbol{y}| = \boldsymbol{1.5}$ mm) with $\boldsymbol{y}$-coordinate parallel to crystal's X-axis ($\boldsymbol{\theta = 0}$) and $\boldsymbol{x}$-coordinate parallel to X+90° ($\boldsymbol{\theta = 90°}$). Period of IDTs in both directions are adapted to achieve common frequency. Magnitude $\widehat{\boldsymbol{u_z}}(\boldsymbol{x,y})$ (a) and phase $\boldsymbol{\varphi_z(x,y)}$ (b) of complex SAW amplitude measured with LDV at f=32.4 MHz.

SAW Polarization Conversion

Besides the spatial distribution of displacement amplitude components $\boldsymbol{u}(x,y) = (u_x, u_y, u_z)$, the polarization at the surface is another characteristic feature for the application of SAW. In particular, microfluidic actuators mainly deploy SAW with large surface normal displacement u_z (Rayleigh SAW) in order to ensure the transfer of momentum from the substrate surface to the fluid (cf. Fig. 1). A major drawback arises due to parasitic transfer of acoustic energy from the SAW to the microfluidic vessel that is needed to confine the fluid volume in real devices. This issue is particularly pronounced for Rayleigh SAW und lowers the device performance. Recently, we proposed an alternative concept based on the deployment of SAW with shear-horizontal polarization, that suffers considerably less attenuation during transmission of vessel walls, but needs to be converted inside the vessel to increase surface normal displacement component [4]. To meet this goal, the SAW polarization has to manipulated during wave propagation, which can be achieved by, e.g. a metal thin film that locally changes the electric boundary condition, causing the electric potential to vanish above the substrate.

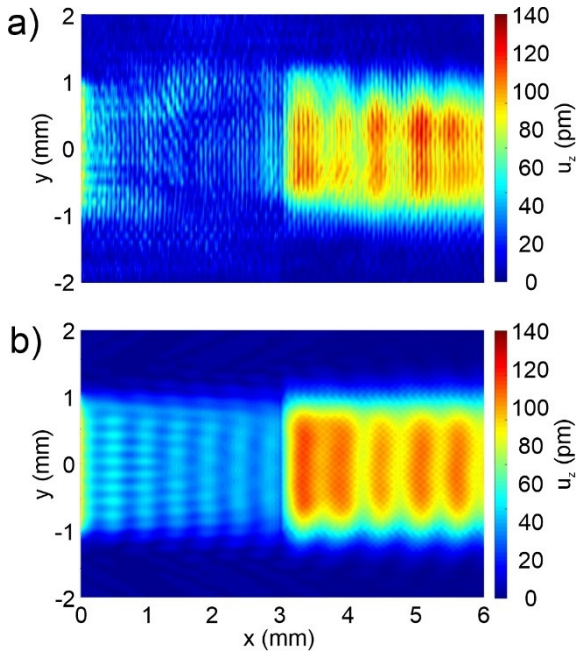

Figure 6: Surface normal displacement amplitude $\boldsymbol{u_z(x,y)}$ for SAW on 64°YX $LiNbO_3$ excited by an IDT with period λ=120 µm. IDT is located at $\boldsymbol{x < 0}$, i.e. SAW propagation direction is from left to right, with free substrate surface at $\boldsymbol{x < 3}$ mm and metallized substrate surface at $\boldsymbol{x > 3}$ mm. Magnitude of SAW amplitude $\widehat{\boldsymbol{u_z}}(\boldsymbol{x,y})$ is evaluated at frequency f=37 MHz: a) LDV measurement, b) FEM simulation. An equivalent voltage was applied to all samples for both experiment and simulation.

In the presence of a surface metallization on 64°YX $LiNbO_3$, surface normal amplitude u_z strongly increases within a distance of about 2–3 wavelengths after the SAW passes the transition from free to metallized surface (Fig. 6). Computations reveal that this effect basically emerges due to the change in electrical boundary conditions induced by the metal film, which fully screens the piezoelectric substrate, so that the electric field accompanying the SAW no longer penetrates outside the substrate. Hence, the abruptly changing boundary conditions of SAW propagation lead to a change of polarization [4].

The presented approach provides two key advantages for SAW-driven microfluidics: The attenuation of the SAW during the transmission of vessel walls is significantly reduced and the lateral position of momentum transfer, i.e., the radiation of bulk waves into the fluid, and so the location of SAW-based manipulation, inside the microfluidic vessel can be easily and precisely defined by means of layout.

References

[1] Weser, R., et al.: The complexity of surface acoustic wave fields used for microfluidic applications. Ultrasonics 106 (2020), 106160

[2] Weser, R, et al.: Experimental and numerical investigations of mechanical displacements in surface acoustic wave bounded beams. Ultrasonics 106 (2020), 106077

[3] Weser, R., et al.: In situ surface acoustic wave field probing in microfluidic structures using optical transmission interferometry. J. Appl. Phys. 129 (2021), 244503

[4] Weser, R, et al.: Polarization manipulation of surface acoustic waves by metallization patterns on a piezoelectric substrate. Appl. Phys. Lett. 117 (2020), 143503